

SPONTANEOUS PRECIPITATION FROM ELECTROLYTIC SOLUTIONS

H. Fűredi-Milhofer

Laboratory for Precipitation Processes, "Rudjer Bošković" Institute, 41000 Zagreb, Yugoslavia

Abstract - The properties of precipitates formed by spontaneous precipitation from electrolyte solutions are determined by the mechanisms and relative rates of precipitation processes (nucleation, crystal growth, aggregation, Ostwald ripening and phase transformation). These again are determined by thermodynamic and kinetic factors and by specific chemical interactions at the solid/solution interface. The mechanism of nucleation determines the number of particles generated which influences the course of subsequent events. Thus, heterogeneous nucleation may be followed by a measurable period of crystal growth and subsequent aggregation and/or recrystallization. The number of nuclei and primary particles generated by homogeneous nucleation is larger by several orders of magnitude and consequently these particles enlarge primarily by aggregation, or else are stabilized by repulsion forces. Thus, hydrophobic precipitates form colloid dispersions, while hydrophilic precipitates tend to form highly hydrated, poorly crystalline precursors. Theoretical considerations point to the most important experimental parameters: the solution composition, the temperature and the reaction time. Stationary state experiments give information on 1) the influence of the solution composition on precipitate properties, 2) the prevailing heterogeneous and homogeneous equilibria at the solid/solution boundary and 3) the critical supersaturation for homogeneous nucleation. Two types of kinetic curves are represented: those pertaining to precipitation (initiated by heterogeneous nucleation) of a single phase are continuous and sigmoidal; the corresponding log rate v.s. log supersaturation curves may be interpreted in terms of the dominant precipitation processes. The formation and transformation, of a metastable phase is characterized by a two-step kinetic curve; the first step corresponds to the precipitation of the precursor, the second step shows secondary precipitation of the next more stable phase.

INTRODUCTION

The basic principles of precipitation of solids from liquids have been applied in classical and nuclear technology, environmental sciences, biomedical research, corrosion, etc.

In some cases precipitation is a process to be avoided (sedimentation and scaling, pathological mineralization of biological tissue) in others to be promoted (separation of trace elements), mostly it is important to control the properties of precipitates.

In this paper attention is given the physico-chemical parameters determining the properties of precipitates which are formed spontaneously, i.e. "ab novo" in electrolyte solutions. It will be shown that precipitation proceeds by succession and interplay of several precipitation processes, i.e. nucleation, growth, aggregation (or stabilization) and ageing. Clearly, the properties of precipitates depend on the mechanisms of those processes, which are rate determining under given circumstances. Therefore, it will be our task, to first explore the general principles, which determine the rates and mechanism of precipitation processes. It will then be shown, how these findings relate to the number, size and

shape of precipitate particles. Finally some useful experimental approaches will be discussed.

THEORETICAL CONSIDERATIONS

Nucleation (1, 2)

The event by which a new phase is formed is called nucleation. It is usual to differentiate between homogeneous nucleation, i.e. the formation of three-dimensional nuclei from a homogeneous parent phase and heterogeneous nucleation, i.e. the growth of nuclei upon specific substrates or nonspecific impurity particles.

Homogeneous nucleation. In classical, thermodynamic nucleation theory the homogeneous nucleus is conceived as an aggregate of critical size which is in unstable equilibrium with its parent phase. It is assumed that macroscopic properties may be assigned to such a nucleus. The radius of the critical cluster, r^* and the activation energy ΔG^* , are given by

$$r^* = - 2 \sigma_{S/L} \bar{v} / kT \ln S \quad (1)$$

and

$$\Delta G^* = 16 \pi \sigma_{S/L}^3 \bar{v}^2 / 3k^2 T^2 \ln^2 S \quad (2)$$

where $\sigma_{S/L}$ is the solid/solution interfacial energy, \bar{v} is the molecular volume, k is the Boltzmann constant and S is the supersaturation defined as

$$S = (a/a_s)_{T,p} \quad (3)$$

a and a_s are the activities of the solute in supersaturated solution and at equilibrium respectively.

The rate of homogeneous nucleation, J , is regarded as the rate of addition of the postcritical ion to the critical nucleus. For stationary conditions J is given by

$$J = (dN/dt)l/V = A_k \exp(-\Delta G^*/kT) \quad (4)$$

where N is the number of nuclei produced per unit time t and unit volume V and A_k is a composite term which is generally taken as $\sim 10^{25}$. Inserting eqn. (2) into (4) we obtain

$$J = A_k \exp(-16 \pi \sigma_{S/L}^3 \bar{v}^2 / 3k^2 T^2 \ln^2 S) \quad (5)$$

Eqn. (5) shows the rate of homogeneous nucleation being an exponential function of the supersaturation. It follows that J is negligible until a certain critical supersaturation, S^* is reached, above which nucleation becomes extremely fast.

If the critical nucleation rate is assigned a value (usually 1 nucleus per sec. per unit volume), and eqn. (5) is rearranged, we obtain for the critical conditions

$$\sigma_{S/L} = (3 k^2 T^2 \ln A_k \ln^2 S^* / 16 \pi \bar{v}^2)^{1/3} \quad (6)$$

Thus, if S^* can be determined by experiment, eqn. (6) may be used to obtain the interfacial energy, $\sigma_{S/L}$, of the nucleus/solution interface. It is then also possible to calculate the critical radius and activation energy from eqns. (1) and (2).

Heterogeneous nucleation. The energetics of heterogeneous (surface) nucleation may be assessed by considering the interaction energies, E_{AA} between ions or molecules of the adsorbent and E_{AS} between adsorbent and substrate ions or molecules respectively. The lattice parameters of the nucleating phase, l_A and the substrate, l_S must also be considered. If E_{AA} and E_{AS} are comparable and the distances l_A and l_S are reasonably close nucleation is said to be coherent (3). Hence, the critical supersaturation and activation energy may be considerably lower than in homogeneous nucleation. In the ideal case, for large E_{AS} no nucleation barrier would exist at all and epitaxial growth could proceed at any supersaturation.

Number and size of precipitate particles. The theories of heterogeneous and homogeneous nucleation imply some conclusions about the relation of the supersaturation and the number and size of precipitate particles.

Since most precipitation reactions are carried out in the presence of impurities, precipitation will commence at supersaturations much lower than the critical supersaturation for homogeneous nucleation. With increasing supersaturation the number of particles stays constant or (in case of varying nucleating efficiency of the impurity particles) increases up to the maximum number of nucleating particles ($N \sim 10^6 - 10^7$ particles per cm^3 or lower). As a consequence particle sizes either increase or slightly decrease with increasing supersaturation. When the critical supersaturation of homogeneous nucleation is exceeded an abrupt increase in the number of particles (by several orders of magnitude) and corresponding (sharp) decrease in their sizes is expected. This particle size maximum has been found in many experimental systems (Figs. 2 and 3).

Crystal growth

Crystal growth may be conceived as a succession of events: 1) transport of ions through the solution, 2) adsorption at the crystal/solution interface, 3) surface diffusion, 4) reactions at the interface (nucleation, dehydration) and 5) incorporation of the reaction products into the crystal lattice. The rate of crystal growth is controlled by the slowest of these processes and therefore much attention has been given the evaluation of kinetic experiments in terms of the rate controlling mechanism.

The rate of precipitation is a function of the available surface area and the supersaturation, i.e.

$$d\alpha/dt = k_f A (c_t - c_s)^p \quad (7)$$

where A is the surface area and c_t and c_s are the solute concentrations at time t and at equilibrium respectively. The fraction of solute precipitated, α , is given by

$$\alpha = (c_0 - c_t) / (c_0 - c_s) = V_t / V_{\max} \quad (8)$$

where c_0 is the initial solute concentration and V_t and V_{\max} are the volumes of the precipitate at

time t and at equilibrium.

For a sufficiently narrow (and constant) distribution of sizes and shapes of particles an average surface area, \bar{A} , may be defined as

$$\bar{A} = \beta N (V_t/N)^{2/3} = \beta N^{1/3} V_t^{2/3} = k_2 N^{1/3} \propto 2/3 \quad (9)$$

where β is a shape factor, N is the number of particles and $k_2 = \beta V_{\max}^{2/3}$ is constant for any given initial solute concentration. Inserting eqn. (9) into eqn. (7) we obtain for the rate of precipitation:

$$d\alpha/dt = K N^{1/3} \propto 2/3 (c_t - c_s)^p \quad (10)$$

If the number of particles is constant, the linear rate of growth may be defined as

$$d\alpha/dt \propto^{-2/3} = R = K' (c_t - c_s)^p \quad (11)$$

where K' includes all constants and $(c_t - c_s)$ is the supersaturation.

Relations of the form of eqn. (11) have been found applicable to many different systems and have been interpreted in terms of crystal growth controlled by a surface process. Attention has centered around the value and meaning of p (for a review see ref. (4)). Obviously, for better understanding the existing crystal growth theories must be considered.

In order to explain crystal growth at extremely low supersaturations, the formation of growth spirals on the crystal surfaces was proposed (5). This screw dislocation controlled growth gives a parabolic dependence of the rate on the supersaturation at low, and a linear dependence at higher supersaturations (6).

At somewhat higher supersaturations crystal growth may be surface nucleation controlled. It was first proposed (7) that crystals are formed through a layer-by-layer mechanism, where each new layer originates in one surface nucleus. This mononuclear growth model has a particularly unfavorable energy requirement.

A number of recent crystal growth theories (4, 8, 9) are based on the polynuclear growth model. According to this model crystal growth is surface nucleation controlled, but the time of nucleation is shorter than the time needed to fill up a monolayer. Then new layers may start before the underlying layers are complete and the surface is at all times covered by surface nuclei, spreading themselves and intergrowing.

Quantitative kinetic treatments (8, 9) are based on the classical theory of heterogeneous nucleation and take into account surface migration of the ions to and their capture at the nucleating site. Lewis (8) proposed the following equation for the linear rate of polynuclear growth:

$$R = (4C)^{1/3} (S' - 1) F_o x_s^{4/3} \exp(-* \Delta G''/3kT) \quad (12)$$

where S' is the supersaturation defined as F/F_e , the ratio between the actual and equilibrium incident fluxes respectively ($S' \sim S$ for an electrolyte solution), $F_o = \zeta F_e$ (ζ is a retardation factor) and $(S' - 1)F_o = R_\infty$ is the maximum rate above which growth is uninhibited by the polynuclear

mechanism. C is a composite term which equals 1 in an order of magnitude approximation. The activation energy for two-dimensional nucleation, $^* \Delta G''$ is given by

$$^* \Delta G'' = \beta'^2 / 4kT \ln S' \quad (13)$$

where β' is a term which includes the edge energy of the two-dimensional nucleus.

Inserting eqn. (13) into (12), putting $C = 1$ and the preexponential factor equal to $K'' R_\infty$, we obtain in the logarithmic form (2):

$$\log R = \log K'' R_\infty - 0.015 \beta'^2 / kT^2 \log S' \quad (14)$$

Eqn. (14) may be compared to the logarithmic form of eqn. (11). Although the supersaturations are expressed differently it is nevertheless obvious that the exponent p in eqn. (11) is related to the edge energy of the two-dimensional nucleus by

$$p \sim -0.015 \beta'^2 / kT^2 \quad (15)$$

Thus, we can see that apart from the supersaturation the material parameters of the crystal (edge energy and diffusion distance) are responsible for its growth kinetics.

An alternative treatment by Nielsen (9) relates the linear rate of growth to the supersaturation and the crystal size. It is important to note that both mentioned treatments predict finite supersaturations at which a changeover in the rate controlling mechanism takes place.

At supersaturations above which polynuclear growth ceases to be rate controlling, transport through the solution becomes the rate controlling mechanism. This mechanism leads to the formation of dendritic crystals (2, 9).

Aggregation and stabilization

The theory of rapid aggregation as given by von Smoluchovski (10) applies to originally monodisperse hydrosols when the movement of particles is due to Brownian motion and no repulsion forces are effective, i.e. each collision leads to permanent contact. Then a dispersion with originally N_0 particles per cm^3 reduces to N_t particles at time t , where

$$N_t = N_0 / (1 + 4 \int_0^t D r N_0 dt) \quad (16)$$

and D is the diffusion coefficient. For aqueous dispersions at 25°C the time required to reduce the particle by half

$$t_{1/2} \sim 2 \times 10^{11} / N_0 \text{ sec} \quad (17)$$

The rate of aggregation is given by

$$dN/dt = -4kT/3 \eta N^2 \quad (18)$$

where η is the fluid viscosity. For heterogeneous hydrosols (11)

$$dN/dt = - A_1 kT/3 \eta N^2 \quad (19)$$

where $A_1 > 4$ is a function of the size distribution. The rate of aggregation further increases under forced convection (shaking, mixing).

We shall now estimate under what conditions rapid aggregation is likely to occur in a precipitation system. A dispersion of newly formed primary particles may be conceived as originally monodisperse. Then for heterogeneous nucleation with a maximum of $10^6 - 10^7$ particles per cm^3 , $t_{1/2} \sim 2 \times 10^4 - 2 \times 10^5$ sec. Apparently in such systems aggregation is not significant in the early stages of precipitation but will be preceded by crystal growth. However, since all impurities may not catalyze nucleation equally well, after a certain time the precipitate will have become polydisperse and the rate of aggregation increases. The effect becomes significant under isoelectric conditions or in the presence of a coagulating electrolyte and eventually influences the rate of crystal growth.

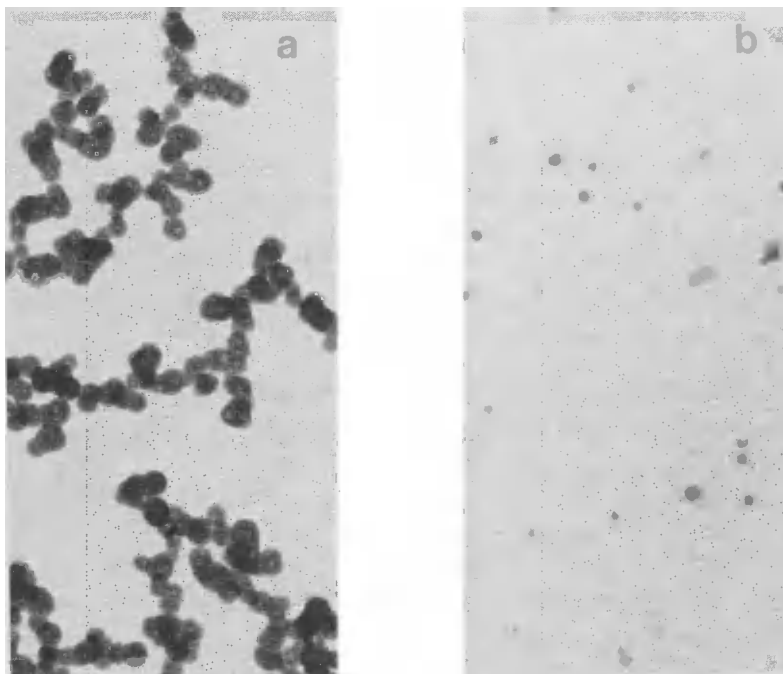


Fig. 1. Electron micrographs of calcium phosphate precipitated at neutral pH a) without additives, b) in the presence of 0.4 mg cm^{-3} of gelatin. After ref. 13.

If precipitation is initiated by homogeneous nucleation the number of particles generated is larger by several orders of magnitude and the half time of aggregation falls within the time scale predicted for nucleation induction periods (2). Thus aggregation of nuclei of primary particles should occur parallel to or immediately after their formation unless the particles are stabilized by an electrical double layer. We may then expect that in systems generated by homogeneous nucleation particles primarily enlarge by aggregation rather than by crystal growth. This is in accordance with the concepts of Težak (12), who conceived embryos, nuclei and primary particles as being formed by aggregation of complex solution constituents (ion pairs, mononuclear and polynuclear complexes). In the course of their formation primary particles develop an electrical double layer and may thus become constituents of stable hydrosols or, under different experimental conditions, enlarge into secondary structures (spherulitic ag-

gregates, mosaic crystal, etc.). An example for the formation of spherulitic aggregates by this mechanism is shown in Fig. 1 (after ref. 13) Fig 1a shows spherulites, which are typically observed when amorphous calcium phosphate is precipitated at neutral pH. The electrophoretic mobility of such particles is close to zero. In the same system much smaller, (probably primary) particles are obtained in the presence of a surface active substance (Fig. 1b).

Ageing

The term ageing is commonly used to describe all, not yet mentioned, physical and chemical changes which a precipitate undergoes in contact with the mother liquid or after liquid has been removed. One such well known phenomenon is

Ostwald ripening. Any two - phase system consisting of a polydisperse precipitate in contact with its mother liquid will be thermodynamically unstable because of its large interfacial energy. A tendency then exists to minimize the excess free energy by coarsening of the particles. A thermodynamic treatment of this phenomenon is given by Kahlweit (14), who sees precipitation of a polydisperse system as a continuous race between the critical radius and the radius of the individual particle. Ostwald ripening has also been demonstrated by computer simulation techniques (15) and both approaches require the process to take place immediately after nucleation. This then is another process besides aggregation, which causes the number of particles to decrease in the initial stages of a precipitation experiment.

Formation and transformation of metastable phases. In a precipitation process in which the formation of several phases is possible, the Ostwald Lussac rule states that the least stable phase with the highest solubility will precipitate first. This is a kinetic phenomenon, i.e. the relative rates of nucleation and growth for the stable and metastable forms will determine which form separates first from solution (16). Considering now eqns. (1) and (5) we conceive that a) the critical radius of the nucleating phase is proportional to its interfacial energy and b) the stationary nucleation rate

$$J \sim 1 / \exp \sigma^3 / S/L \quad (20)$$

Thus the phase with lowest interfacial energy requires the smallest accretion of ions to form a thermodynamically stable nucleus and has the largest nucleation rate. Since the interfacial energy of a substance is inversely proportional to its solubility (17), clearly nucleation of the phase with highest solubility is kinetically favoured.

Numerous examples of such behaviour have been known. Extremely important in biological systems, as well as in industrial practice is the tendency of strongly hydrated cations to form metastable hydrates, such as the higher hydrates of calcium oxalate (18) and poorly crystalline precursors such as amorphous calcium phosphate (13, 19 - 23, Figs. 1, 5) hydrous oxide gels (24) etc. The formation of metastable hydrates is favoured by the large energy requirement for desolvation which may not be easily overcome by electrostatic forces. The formation of highly hydrated, poorly crystalline or amorphous precursors is favoured at relatively high supersaturations, where the critical radius is expected to be small (eqn. 1) and - for crystals of large unit cells - may become smaller than one unit cell. If, as a consequence of homogeneous nucleation, particles enlarge by aggregation rather than by crystal growth (Fig. 1), strongly hydrated cations are likely to form poorly ordered structures, which retain

considerable amounts of molecular water.

Ageing in contact with the mother liquid leading to the transformation of metastable phases frequently involves dissolution of the less stable and reprecipitation of the next more stable form (20, 24, 25). Nucleation of the secondary precipitate is usually heterogeneous with the precursor serving as the nucleating phase (19, 22, 23). Amorphous precipitates may have to undergo internal rearrangements (dehydration, crystal ordering) before effectively nucleating the secondary precipitate (22, 23). Progressive ordering processes in the solid phase, accompanied by the liberation of water and resulting in a more crystalline precipitate have been demonstrated in many hydrous oxide gels (24).

Chemical aspects

So far we have only considered thermodynamic and kinetic aspects of precipitate formation. The chemical composition of the mother liquid may, however, have a decisive role in determining the properties of precipitates (12). Thus it is known, that adsorption of foreign ions at the solid solution interface may reduce the overall growth rate of particles or change their morphology by preferential adsorption (for examples see refs. 23, 26). In some cases adsorption and incorporation of neutral complexes of constituent ions, rather than of single ions was reported to be the dominant mechanism in surface reaction controlled crystal growth (21, 27). It has also been shown (28) that certain anions (Cl^- , SO_4^{2-} , ClO_4^-) may play a decisive role in determining the size and shape of precipitate particles which formed by ageing of solutions. Specific interactions at the solid/solution interface are also responsible for charge reversals of colloid particles, resulting in restabilization of coagulated precipitates (29, 30). Thus the surface charge of colloid particles indeed depends on the concentrations of all ionic species in solution, some of which may be specifically adsorbed. It has been shown for hydrous oxide gels (30), that the change in standard free energy of adsorption of a species i at the solid/solution interface consists of a coulombic, a solvation and chemical free energy term, i.e.

$$\Delta G_{\text{ads},i} = \Delta G_{\text{coul},i} + \Delta G_{\text{sol},i} + \Delta G_{\text{chem},i} \quad (21)$$

The latter term takes care of specific chemical interactions at the interface and cannot be always independently evaluated.

Morphology of precipitate particles.

The number, size and shape of precipitate particles are determined by the mechanisms and relative rates of all precipitation processes. The mechanism of nucleation is of overriding importance in determining the course of subsequent events.

Size and shape. If a relatively stable solid phase is nucleated upon impurity particles, nucleation is followed by a period of crystal growth and (possibly) subsequent aggregation. The size and shape of precipitate particles is then determined by the rate controlling crystal growth mechanism, which depends on the supersaturation (8, 9). At low supersaturations we expect the formation of compact crystals (also needles or platelets if growth is anisotropic (8)) as a result of a polynuclear growth mechanism. At medium supersaturations dendrites may be formed by bulk diffusion controlled growth (9). The picture may be complicated by the formation and transformation of metastable precursors.

At high supersaturations where nucleation is prevalently homogeneous, a drastic change in morphology occurs. Hydrophobic precipitates form colloid dispersions or coagulates, while hydrophilic precipitates tend to form highly hydrated, poorly crystalline precursors, which undergo transformations into crystalline precipitates (33).

Number of particles. The change in the number of particles with supersaturation has been predicted by nucleation theory. However, the number of particles observed after homogeneous nucleation may be significantly smaller than expected. For any experimental tool there exists a certain lower limit of particle sizes which may be detected. When particles were generated by homogeneous nucleation this size is reached primarily by aggregation. Thus the original number of particles may be larger by orders of magnitude than the number of particles actually counted (Fig. 1, and refs. 21, 23). Ostwald ripening effects the number of particles in the same direction (14). Consequently, extreme caution should be utilized if evaluating particle counts of precipitates generated by homogeneous nucleation.

EXPERIMENTAL APPROACH

According to the foregoing consideration the properties of precipitates are determined by the following experimental parameters: 1) the solution composition (reactant concentrations, pH, ionic strength, foreign ions and molecules), 2) the temperature and 3) the reaction time. Information on the influence of these parameters is obtained by systematic stationary state and kinetic experiments.

Stationary state experiments

The objective of such experiments is to investigate changes of precipitate properties within a large range of concentrations (activities) of reactants and/or additives. The reaction time is kept constant and long enough to allow a stationary state to be established. Concentrations are changed in discreet steps, which is achieved by mixing together (in a reproducible manner) stable solutions containing different, known reactant concentrations. Once formed, precipitates are aged for a predetermined time and one or more characteristic features (morphology, turbidity, etc.) are observed. The data may be represented in the form of precipitation curves (Fig. 2) and diagrams (Fig. 3). Such diagrams give information on the influence of solution composition on the properties of precipitates and on the prevailing solid/solution equilibria (12, 31, 32).

They also enable the determination of the critical supersaturation for homogeneous nucleation (33) and subsequent calculations of the interfacial energy and radius of the homogeneous nucleus (eqns. 1 and 6). Precipitation curves are plots of a measured quantity, X , against the concentration (activity) of one component (A) at constant concentration (activity) of the other (B). A set of such curves is shown in Fig. 2 (after ref. 33).

The results shown in this figure are a typical example of the effect of changes in the mechanisms of nucleation and crystal growth on the number, size and shape of precipitate particles. Apparently within the heterogeneous nucleation region the crystal growth mechanism changed from surface reaction controlled (region P) to diffusion controlled (region D). The subsequent drastic change in morphology and abrupt decrease in particle sizes (region M), resulting in the appearance of a typical particle size maximum, indicates the onset of homogeneous nucleation. The corresponding increase in the number of

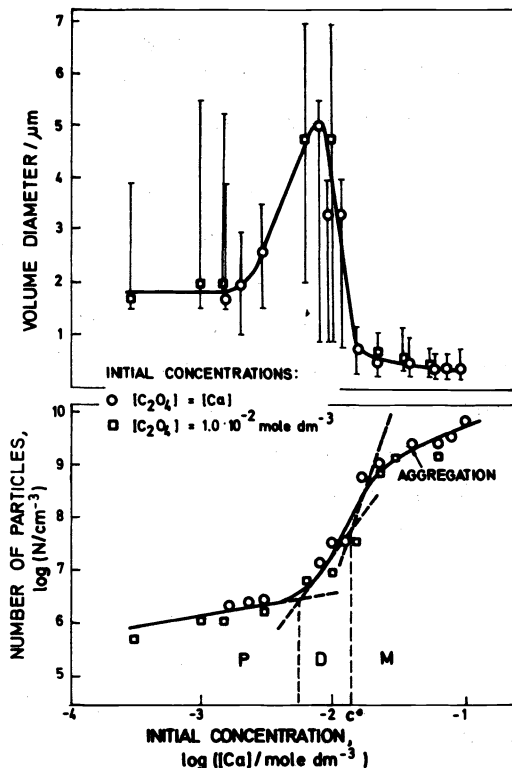


Fig. 2. Precipitation of calcium oxalate from concentrated electrolyte solutions (0.3 mole dm^{-3} sodium chloride, pH 6.5, 25°C , $t = 10 \text{ min.}$, Coulter Counter). Precipitation curves show changes in the number of particles per cm^3 ($>0.5 \mu\text{m}$, lower diagram) and the corresponding populated range of particle sizes (upper diagram) as a function of the initial reactant concentrations. Points in the upper diagram represent population maxima. Prevailing morphological types: Platelets and octahedral bipyramids (P), dendrites (D) and microcrystalline aggregates (M). c^* - critical concentration for homogeneous nucleation. After ref. 33.

particles is smaller than expected by nucleation theory, the reasons being aggregation and the detection limit of the instrument. A distinct inflection on the number/concentration curve is nevertheless apparent. All these data are sufficient to obtain a reasonable estimate of c^* , from which the critical supersaturation for homogeneous nucleation can be calculated.

A precipitation diagram is a plane showing contours of equal values of a chosen experimental parameter, X , as a function of the initial concentrations (activities) of precipitation components A and B. The contours may be replaced by boundaries of concentration regions, within which precipitates with similar characteristic properties prevail. Such a diagram may be constructed from a set of precipitation curves with different constant initial concentrations of one of the components. An example is shown in Fig. 3.

Part of any precipitation diagram is the precipitation boundary (PB) which is defined as the boundary between clear solutions and detectable precipitates. Its position depends on the time and tool of observation. In a quasi-equilibrium situation the PB may practically coincide with the solubility limit and its position then reflects the prevailing heterogeneous equilibria in the system (12, 31, 32). For instance the PB represented by line 1 in Fig. 3 follows the ionic solubility product of silver chloride and we therefore conclude, that in this concentration region complex formation is negligible. More generally, under stationary state conditions, the PB is shifted towards higher supersaturations, deviding thus the

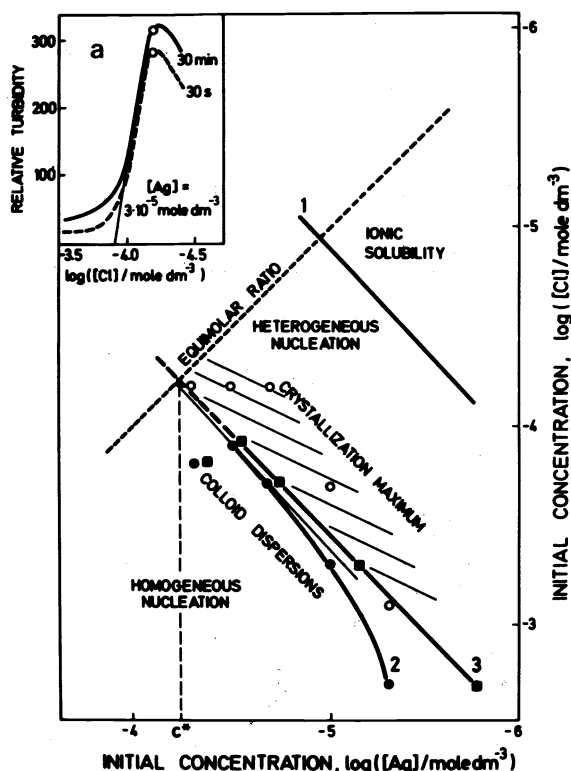


Fig. 3. Section of precipitation diagram of silver chloride constructed from a series of turbidimetric precipitation curves with different constant concentrations of silver ions (ref. 34, Fig. 3a). Line 1: precipitation boundary (after ref. 31); full dots and curve 2: concentration products at the onset of homogeneous nucleation; full squares and line 3: corresponding calculated activity products. The concentration products were obtained from the intersections of tangents to turbidity curves with the abscissa, as shown in Fig. 3a. c^* - critical ionic product for homogeneous nucleation. After ref. 33.

region of metastable solutions (where crystal growth may be induced by specific seed crystals) from the region of spontaneous precipitation. Such boundaries yield information pertaining to mononuclear crystal growth kinetics (35).

The boundary between the regions within which precipitates are generated by heterogeneous and prevalently homogeneous nucleation respectively (lines 2 and 3 in Fig. 3) in most precipitation diagrams appears as a discontinuity, which may be recognized by turbidimetry, morphological observations or other means. Such boundary may then be used to determine the critical supersaturation for homogeneous nucleation as an average value over a wide range of initial reactant concentrations (33), the procedure is shown in Fig. 3. The appearance of a particle size maximum, preceding the onset of homogeneous nucleation (crystallization maximum (34) in Fig. 3) is in accordance with the requirements of nucleation theory.

Kinetic studies

Kinetic studies show which of the precipitation processes are rate determining under a given set of experimental conditions and yield information on the rates and mechanisms of some of these processes. The basis of a kinetic analysis is the progress curve, showing changes of the solute concentration or the amount of solid phase formed as a function of time. Usually the interpretation of such curves requires several experimental techniques, a combination of solution analysis with techniques giving

information on the properties of precipitates (particle number and size analysis, morphology and physicochemical characterization) is advantageous. A discussion of methods and techniques commonly used to obtain and interpret progress curves is given elsewhere (2, 36).

Fig. 4 shows a progress curve and the corresponding log rate v.s. log supersaturation curve, both typical for a precipitation process initiated by heterogeneous nucleation during which phase transformation is negligible. An analysis of the rate v.s. supersaturation curve (lower diagram) according to

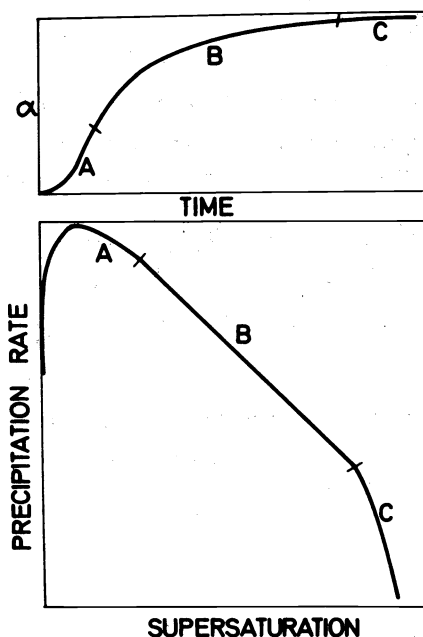


Fig. 4. Schematic α v.s. time curve (upper diagram) and the corresponding rate v.s. supersaturation curve (lower diagram, log/log scale, the rate is corrected by $\alpha^{-2/3}$) obtained when calcium hydrogen phosphate dihydrate (38) or calcium oxalate trihydrate (39) were precipitated from concentrated sodium chloride solutions (0.15 and 0.3 mole dm^{-3}). Phase transformation was negligible during the runs. Sections A, B and C in both diagrams are corresponding in time. A - nucleation and growth, B - crystal growth, C - growth and aggregation or dissolution/recrystallization.

eqn. (10) implies the following interpretation:

Nucleation and growth in the initial stages of precipitation causes a sharp increase in the number of growing particles and corresponding increase in the precipitation rate. At the same time the supersaturation decreases, causing the process to slow down. Consequently a maximum (section A in Fig. 4) appears on the rate v.s. supersaturation curve (compare also ref. 37). For a monodisperse system the time corresponding to the maximum (from the inflection on the α/t curve) should coincide with the time of the onset of precipitation, the breadth of the maximum is due to polydispersity. The linear part on the rate v.s. supersaturation curve (section B) shows that in this section the requirements of eqn. (11) are fulfilled, i.e. $N \sim \text{const.}$ and $\bar{A} \sim \alpha^{2/3}$. Consequently p may be determined and interpreted in terms of any of the crystal growth theories. Subsequent deviation from linearity (section C) shows that in addition to crystal growth another process (dissolution/recrystallization or aggregation) has become significant, causing the precipitation rate to decrease faster than expected from eqn. (11).

In order to differentiate between the two possibilities (recrystallization and aggregation) further analysis of section C is required. One criterion could be the dependence of the number of particles on time. If the deviation from linearity was caused by aggregation, a plot of $1/N$ v.s. time should give a straight line with the slope proportional to the size distribution (eqns. (18) and (19)). If, however, crystal growth is slowed down primarily by recrystallization, useful information should be obtained by studies of the heterogeneous exchange of radionuclides (20, 40).

Plots of the type shown in Fig. 4. have been consistently obtained when calcium hydrogenphosphate dihydrate (DCPD, ref. 38) and calcium oxalate trihydrate (COT, ref. 39) were precipitated from concentrated sodium chloride solutions (0.15 and 0.3 mole dm^{-3}). In the DCPD system the shape of the individual rate v.s. supersaturation curves depended on the supersaturation; at very low supersaturations section C did not appear, while above a certain supersaturation no linear dependence of the rate on the supersaturation was obtained at all.

For the COT system linear plots of $1/N$ v.s. time were obtained when particles were counted during the time interval, corresponding to sections C of the log rate v.s. log supersaturation curves (compare Fig. 4). The deviation from the course of the growth curve was therefore attributed to a loss in surface area due to aggregation (41).

Fig. 5 shows a set of schematic, discontinuous kinetic curves (turbidity, reactant concentrations and pH v.s. time), which reflect the formation of a metastable precursor and secondary precipitation of the next more stable phase.

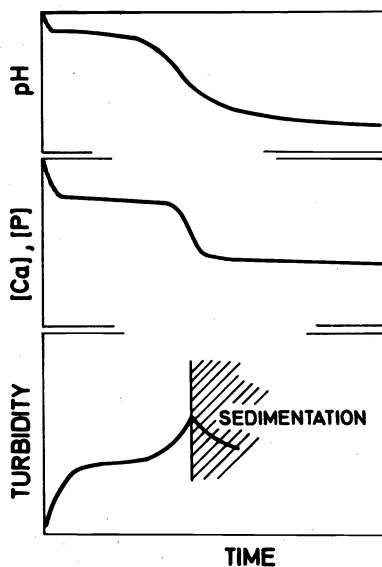


Fig. 5. Schematic turbidity, reactant concentrations and pH v.s. time curves which characterize the kinetics of precipitation of calcium phosphates in the region of prevalently homogeneous nucleation (19 - 23). The two-step form of the curves indicates the formation of a precursor (amorphous calcium phosphate) and subsequent precipitation of the next more stable phase.

Progress curves of this type characterize the formation and transformation of amorphous calcium phosphate (ACP; 19 - 23) and other metastable hydrates such as COT (18), $\text{CaSO}_4 \times 1/2 \text{H}_2\text{O}$ (4), etc. The complex reaction sequences which take part in such precipitation processes require detailed kinetic analyses of each time period, employing combinations of as many experimental techniques as possible.

An investigation of the formation and transformation of ACP particles by a combination of solution and particle morphology and size analysis shows that 1) ACP spherules (Fig. 1a) are formed by prevalantly homogeneous nucleation and subsequent aggregation of primary particles, 2) such spherules grow by a surface controlled mechanism, 3) the next more stable phase is formed by heterogeneous nucleation upon the precursor particles. Details of this investigation will be given in another paper at this Conference (23).

CONCLUSIONS

Thermodynamic, kinetic and chemical aspects of precipitate formation have been considered. It is shown that the gross properties of precipitates are influenced by the number of nuclei initially generated (i.e. the mechanism of nucleation) because this property determines whether crystal growth or aggregation/stabilization will be dominant in the early stages of precipitation. Theoretical considerations point to the most important experimental parameters, which determine the properties of precipitates, i.e. the solution composition, the temperature and the reaction time. Stationary state experiments give information on: 1) the influence of the solution composition on the properties of precipitates, 2) the prevailing heterogeneous and homogeneous equilibria in the system and 3) the critical supersaturation for homogeneous nucleation, from which the interfacial energy and radius of the homogeneous nucleus can be calculated. Precipitation in a system with a reasonably narrow and constant distribution of sizes and shapes of particles is described by the general kinetic equation

$$d\alpha / dt = KN^{1/3} \alpha^{2/3} (c_t - c_s)^p \quad (1)$$

where α is the fraction of solute precipitated, N is the number of particles, c_t and c_s are solute concentrations at time t and at equilibrium and K and p are constants. A log rate v.s. log supersaturation plot interpreted in terms of eqn. (1) gives information on the precipitation processes, which are rate controlling within a certain time period.

REFERENCES

1. A.G. Walton, in Nucleation, A.C. Zettlemoyer editor, 225 - 307, Marcel Dekker, New York (1969).
2. H. Fűredi-Milhofer and A.G. Walton, in Dispersions of Powders in Liquids 3th edition. G.D. Parfitt, editor, Applied Science, Barking, Essex, in press.
3. R.J.H. Voorhoeve, Surface Sci. **28**, 145 - 156 (1971).
4. G.H. Nancollas, Adv. Colloid Interface Sci. **10** 215-252 (1979).
5. F.C. Frank, Disc. Faraday Soc. **5**, 48 - 54; 67 - 79 (1949).
6. W.K. Burton, N. Cabrera and F.C. Frank, Phil. Trans. Royal Soc. London A **243**, 299-358 (1951).
7. I.N. Stranski, Z. Phys. Chem. A **136**, 259 (1928).

8. B. Lewis, J. Crystal Growth **21**, 29 - 39; 40 - 50 (1974).
9. A.E. Nielsen, Kinetics of Precipitation, Pergamon, Oxford, (1964).
10. M. von Smoluchovski, Z. phys. Chem. **92**, 129 (1917).
11. D.L. Swift and S.K. Friedländer, J. Colloid Sci. **19**, 621 - 646 (1964).
12. B. Težak, Disc. Faraday Soc. **42**, 175 - 186 (1966).
13. H. Füređi-Milhofer, Lj. Brečević, E. Oljica, Z. Gass and G. Perović in Particle Growth in Suspension, A.L. Smith, editor, 109 - 120, Academic Press, London (1973).
14. M. Kahlweit, in Physical Chemistry **10**, 719 - 759, Academic Press, New York (1970); Adv. Colloid Interface Sci. **5**, 1 - 35 (1975).
15. D. Robertson and G.M. Pound, J. Crystal Growth **19**, 269 - 284 (1973).
16. I.N. Stranski and D. Totomanov, Naturwissenschaften **20**, 905 (1933).
17. A.E. Nielsen and O. Söhnel, J. Crystal Growth **11**, 233 - 242 (1971).
18. B. Tomažić and G.H. Nancollas, Invest. Urol. **16**, 329 - 335 (1979).
19. Lj. Brečević and H. Füređi-Milhofer, Calc. Tiss. Res. **10**, 82 - 90 (1972).
20. R. Despotović, N. Filipović-Vinceković and H. Füređi-Milhofer, Calc. Tiss. Res. **18**, 13 - 26 (1975).
21. H. Füređi-Milhofer, Lj. Brečević and B. Purgarić, Faraday Disc. Chem. Soc. **61**, 184 - 193 (1976).
22. Lj. Brečević and H. Füređi-Milhofer, in Industrial Crystallization, J.W. Mullin editor, 277 - 283, Plenum, New York (1976).
23. Lj. Brečević and H. Füređi-Milhofer, Fourth Int. Conf. Surface and Colloid Sci., Jerusalem (1981).
24. G.C. Bye and K.S.W. Sing in Particle Growth in Suspensions, A.L. Smith, editor, 29 - 45, Academic Press, London (1973).
25. B. Subotić, D. Škrtić, I. Šmit and L. Sekovanić, J. Cryst. Growth **50**, 498 - 508 (1980).
26. Lj. Brečević and H. Füređi-Milhofer, Calcif. Tiss. Int. **28**, 131 - 136 (1979).
27. A.E. Nielsen, Acta Chem. Scand. **13**, 784 - 802 (1959).
28. E. Matijević, J. Colloid Interface Sci. **43**, 217 - 245 (1973); **58**, 374 - 389 (1977).
29. B. Težak, E. Matijević, K.F. Schulz, J. Kratochvil, M. Mimik and V.B. Vouk, Disc. Faraday Soc. **18**, 63 - 73 (1954).
30. R.O. James and T.W. Healy, J. Colloid Interface Sci. **40**, 65 - 81 (1972).
31. J. Kratochvil, B. Težak and V.B. Vouk, Arhiv kem. **26**, 191 - 209 (1954).
32. H. Füređi, in The Formation and Properties of Precipitates by A.G. Walton, 188 - 215, Interscience, New York (1967).
33. H. Füređi-Milhofer, M. Marković, Lj. Komunjer, B. Purgarić and V. Babić-Ivančić, Croat. Chem. Acta **50**, 139 - 154 (1977).
34. B. Težak, Z. phys. Chem. **192**, 101 - 111 (1943).
35. B. Kosar-Grašić, B. Purgarić and H. Füređi-Milhofer, J. inorg. nucl. Chem. **40**, 1877 - 1870 (1978).
36. H. Füređi-Milhofer, Croat. Chem. Acta **53**, 243 - 254 (1980).
37. E.V. Khamskij, Kristall Technik **8**, 107 - 113 (1973).
38. B. Purgarić and H. Füređi-Milhofer, Proc. Intern. Conf. Colloid Surface Sci. **1**, E. Wolfram, editor, 273 - 280, Akadémiai Kiadó, Budapest (1975).
39. H. Füređi-Milhofer, D. Škrtić, M. Marković and Lj. Komunjer in Urolithiasis: Clinical and Basic Research, L.H. Smith, editor, Plenum, New York, in press.
40. R. Despotović, Disc. Faraday Soc. **42**, 175 - 209 (1966).
41. D. Škrtić, M. Marković and H. Füređi-Milhofer, in preparation.